



Heriot-Watt University  
Research Gateway

## Epitaxial lift-off of II-VI semiconductors from III-V substrates using a MgS release layer

### Citation for published version:

Rajan, A, Davidson, IA, Moug, RT & Prior, KA 2013, 'Epitaxial lift-off of II-VI semiconductors from III-V substrates using a MgS release layer', *Journal of Applied Physics*, vol. 114, no. 24, 243510.  
<https://doi.org/10.1063/1.4859515>

### Digital Object Identifier (DOI):

[10.1063/1.4859515](https://doi.org/10.1063/1.4859515)

### Link:

[Link to publication record in Heriot-Watt Research Portal](#)

### Document Version:

Publisher's PDF, also known as Version of record

### Published In:

Journal of Applied Physics

### General rights

Copyright for the publications made accessible via Heriot-Watt Research Portal is retained by the author(s) and / or other copyright owners and it is a condition of accessing these publications that users recognise and abide by the legal requirements associated with these rights.

### Take down policy

Heriot-Watt University has made every reasonable effort to ensure that the content in Heriot-Watt Research Portal complies with UK legislation. If you believe that the public display of this file breaches copyright please contact [open.access@hw.ac.uk](mailto:open.access@hw.ac.uk) providing details, and we will remove access to the work immediately and investigate your claim.

## Epitaxial lift-off of II–VI semiconductors from III–V substrates using a MgS release layer

Akhil Rajan, Ian A. Davidson, Richard T. Moug, and Kevin A. Prior

Citation: *Journal of Applied Physics* **114**, 243510 (2013); doi: 10.1063/1.4859515

View online: <http://dx.doi.org/10.1063/1.4859515>

View Table of Contents: <http://scitation.aip.org/content/aip/journal/jap/114/24?ver=pdfcov>

Published by the [AIP Publishing](#)

---

### Articles you may be interested in

II-VI heterostructures obtained by encapsulation of colloidal CdSe nanowires by molecular beam epitaxy deposition of ZnSe

*J. Vac. Sci. Technol. B* **29**, 03C102 (2011); 10.1116/1.3547715

Intersubband transitions in molecular-beam-epitaxy-grown wide band gap II-VI semiconductors

*J. Vac. Sci. Technol. B* **25**, 995 (2007); 10.1116/1.2720859

Epitaxial liftoff of ZnSe-based heterostructures using a II-VI release layer

*Appl. Phys. Lett.* **86**, 011915 (2005); 10.1063/1.1844595

Reduced defect densities in the ZnO epilayer grown on Si substrates by laser-assisted molecular-beam epitaxy using a ZnS epitaxial buffer layer

*Appl. Phys. Lett.* **85**, 5586 (2004); 10.1063/1.1832734

II–VI quantum dot formation induced by surface energy change of a strained layer

*Appl. Phys. Lett.* **82**, 4340 (2003); 10.1063/1.1583141

---



**AIP** | Journal of  
Applied Physics

*Journal of Applied Physics* is pleased to  
announce **André Anders** as its new Editor-in-Chief

# Epitaxial lift-off of II–VI semiconductors from III–V substrates using a MgS release layer

Akhil Rajan,<sup>1</sup> Ian A. Davidson,<sup>1,2</sup> Richard T. Moug,<sup>1</sup> and Kevin A. Prior<sup>1</sup>

<sup>1</sup>*Institute of Photonics and Quantum Sciences, SUPA, School of Engineering and Physical Sciences, Heriot-Watt University, EH14 4AS Edinburgh, United Kingdom*

<sup>2</sup>*Department of Physics, Stockholm University, S-10691, Stockholm, Sweden*

(Received 17 September 2013; accepted 12 December 2013; published online 27 December 2013)

Epitaxial lift-off (ELO) is a post-growth process that allows an epitaxial layer to be removed from its original substrate and transferred to a new one. ELO has previously been successfully demonstrated for III–V materials and also ZnSe based II–VI semiconductors using a MgS sacrificial layer. Following the recent successful growth of epitaxial MgS layers on GaP and InP substrates, in this paper we compare ELO of II–VI epilayers grown on GaP, GaAs, and InP substrates using MgS sacrificial layers in the range of 7–15 nm thick. Good quality lifted layers are obtained rapidly from InP and GaAs substrates. For GaP substrates, ELO is much slower and good quality lifts have only been achieved with ZnSe epilayers. Photoluminescence spectra obtained from epitaxial layers before and after ELO show changes in peak positions, which are compatible with changes of strain in the layer. The layers produced by ELO are flat and free of cracks, suggesting that this is an efficient and convenient method for the transfer of II–VI epitaxial layers to other substrates. © 2013 AIP Publishing LLC. [<http://dx.doi.org/10.1063/1.4859515>]

## I. INTRODUCTION

The integration of different semiconductors on a single substrate has been an important research area for many years. Successful growth by a technique such as molecular beam epitaxy (MBE) requires layer deposition on single crystal substrates, but for many applications the substrate serves no role after growth other than as a support for the device and, for some technologies, such as solar cells, using single crystal substrates is simply too expensive. However, epitaxial lift-off (ELO) is a technique that introduces flexibility to the fabrication and integration of semiconductor devices and the potential to reuse substrates. ELO is a post growth process, and is based on the technique first reported in 1978 by Konagai where an epitaxial film was removed from the substrate by etching a thick sacrificial layer.<sup>1</sup> The technique exploits the large difference in etch rates of GaAs and  $\text{Al}_x\text{Ga}_{1-x}\text{As}$  in HF, where for  $x \geq 0.5$ , the etch rate of the  $\text{Al}_x\text{Ga}_{1-x}\text{As}$  is many orders of magnitude faster than that of GaAs. This process was later developed by Yablonovich *et al.*<sup>2</sup> to allow material to be lifted from structures with thinner sacrificial layers by using a wax capping layer deposited on the top of the sample that strains the epitaxial layers during the etching process. This strain causes the etching channel between the substrate and epitaxial layer to remain open and aids the removal of reaction products.

ELO has been used on various III–V structures with light emitting diodes (LEDs),<sup>3</sup> laser diodes,<sup>4</sup> and solar cells<sup>5</sup> all successfully transferred onto foreign substrates. Initially, II–VI layers could not be lifted unless they were deposited on a III–V epitaxial structure that incorporated a sacrificial layer,<sup>6</sup> due to the lack of a compatible II–VI sacrificial material. However, we have since developed an ELO process based solely on II–VI semiconductors in which a zinc blende (ZB) MgS sacrificial layer was etched with dilute HCl. Using this process, we demonstrated ELO of ZnSe/ZnCdSe quantum well structures

from GaAs substrates.<sup>7</sup> Recently, we have successfully grown heterostructures containing ZB MgS on three different III–V substrates: GaP, GaAs, and InP,<sup>8</sup> where the MgS layer has strains ranging from 4.4% (tensile) on InP to –3.0% (compressive) on GaP. In this paper, we demonstrate that ZB MgS can be used as a sacrificial layer in ELO for II–VI heterostructures deposited on all three substrates. To our knowledge, this is the first time that ELO has been successfully performed using the same sacrificial layer over a range of different substrates.

## II. EXPERIMENTAL

All structures were grown by MBE on GaP, GaAs, and InP substrates using the procedures given previously.<sup>8</sup> A sample with the structure: GaAs/ZnSe(50 nm)/MgS(7 nm)/ZnSe(300 nm) was grown first, as successful ELO has been performed on similar structures previously.<sup>7</sup> In this structure, ZB MgS is lattice matched to both GaAs and ZnSe and this structure was, therefore, used as a reference to compare the ELO from other substrates.

On GaP and InP substrates, two different sets of samples were grown. In the first set, the II–VI layers apart from MgS were chosen to have low strains to the III–V substrate. In the second set, the epitaxial layers to be lifted were all ZnSe, which is not lattice matched to either GaP or InP. The two sets of samples deposited on GaP had structures: GaP/ZnS(40 nm)/MgS(7 nm)/X, where X is either a ZnS (200 nm) or ZnSe (250 nm) layer. Similarly, the samples grown on InP had structures InP/Zn<sub>0.56</sub>Cd<sub>0.44</sub>Se(60 nm)/MgS(7 nm)/X, where X is either Zn<sub>0.56</sub>Cd<sub>0.44</sub>Se (300 nm) or ZnSe (300 nm). On these two substrates, some relaxation of the MgS layers will occur during growth, meaning that in both the GaP/ZnS/MgS/ZnS and InP/ZnCdSe/MgS/ZnCdSe structures the strain states of the top and bottom layers will not be identical.

Lift-off was performed on samples,  $\sim 3 \times 3 \text{ mm}^2$  cleaved from the wafer material, taking considerable care to get perfect cleaves. The surface was then coated with Apiezon wax at  $\sim 120^\circ\text{C}$ . The samples were then etched in 30% HCl at room temperature with the wax coated surface uppermost. Once the etch is complete, the wax-coated layer floats to the surface, leaving the substrate behind and facilitating its removal from the etch solution.

Before ELO, symmetric 004 double crystal x-ray diffraction (XRD) rocking curves were obtained using  $\text{Cu } K\alpha_1$  radiation and a Bede 200 diffractometer from all structures grown along [110]. After ELO and transfer to a glass substrate, absorption spectra were obtained using a vertical-VASE ellipsometer system covering the spectral range of 270–800 nm. Photoluminescence (PL) measurements were performed at 77 K on samples before and after ELO using  $\sim 10 \text{ mW}$  excitation from a 405 nm laser diode focused to an  $\sim 6 \mu\text{m}$  diameter spot. As the bandgap of ZnS ( $\sim 3.7 \text{ eV}$ ) is greater than that of the available pump source, the GaP/ZnS/MgS/ZnS structures could not be measured by PL. For all other samples, the emitted light was collected using a fiber coupled 100 mm focal length spectrometer and CCD. The same lens was used both to focus the laser and collect the PL signal.<sup>9</sup> Spectra were typically recorded using an integration time of 10 s.

### III. RESULTS AND DISCUSSION

Double crystal rocking curve 004 spectra are shown in Figs. 1 and 2 for the first and second sets of samples, respectively. In each figure, the positions of all substrate peaks are superimposed and centered at the origin. The curves show peaks from only the thicker buffer and top layers, as the central MgS layer is too thin to produce a resolvable peak. In these structures, the strain between the substrate and epitaxial layers results in some relaxation. This is most obvious in the GaP/ZnS/MgS/ZnS structure, where the different strains in top and bottom layers produce two clearly resolvable

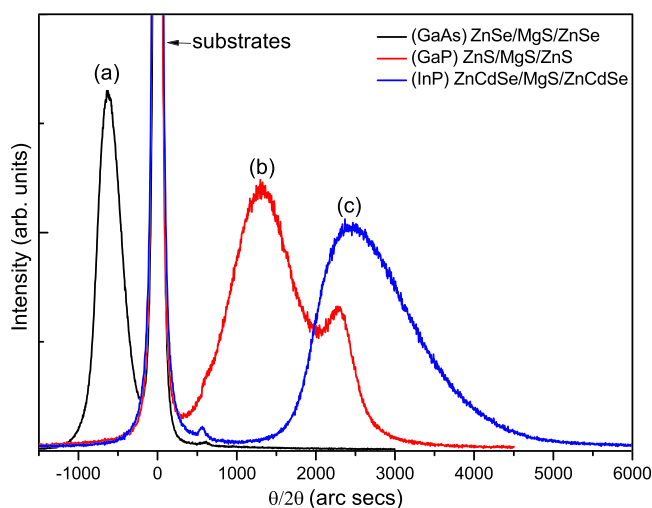


FIG. 1. XRD rocking curves from (a) ZnSe/MgS/ZnSe, (b) ZnS/MgS/ZnS, and (c) ZnCdSe/MgS/ZnCdSe epitaxial layers on GaAs, GaP, and InP substrates, respectively. Reprinted with permission from Appl. Phys. Lett. 102, 032102 (2013). Copyright 2013 AIP Publishing LLC.<sup>8</sup>

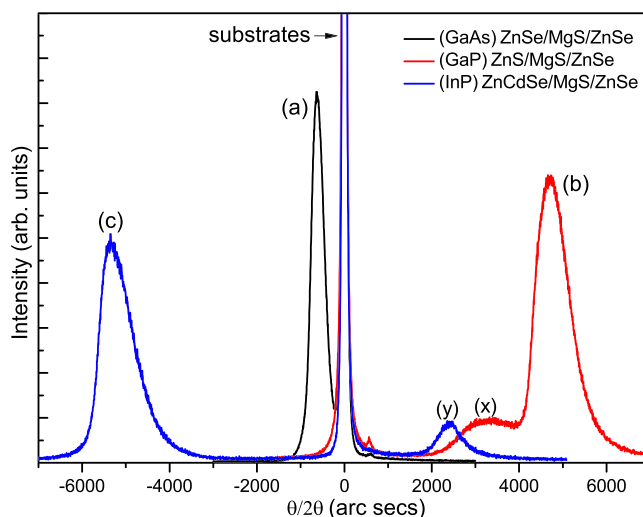


FIG. 2. XRD rocking curves from (a) GaAs/ZnSe/MgS/ZnSe, (b) GaP/ZnS/MgS/ZnSe, and (c) InP/ZnCdSe/MgS/ZnCdSe structures. Peaks from the three substrates have been aligned at the origin. Peaks (a), (b), and (c) are from the ZnSe cap layers for these three structures, whereas (x) and (y) peaks originate from ZnS and ZnCdSe buffer layers, respectively.

peaks. In the InP/ZnCdSe/MgS/ZnCdSe structure, there is one asymmetric peak which is resolvable into two Gaussian components. In set 2, the ZnSe layer peaks were used to calculate the residual strain and layer relaxation. In these structures, the residual strains are small and are comparable in magnitude to the thermal strains introduced on cooling the samples. Removing these thermal strains allows the residual strains and sample relaxations at the growth temperature to be calculated (Table I). This confirms that for the GaP and InP substrates the layers are almost completely relaxed, as expected, while only partial relaxation has taken place on the GaAs substrate, where the ZnSe layer is more closely lattice matched (Table II). In the layer grown on GaP, it can also be seen that the thermal strain is sufficiently large to change the residual strain measured at room temperature from compressive to tensile.

Peaks (a), (b), and (c) are from ZnSe cap layers, whereas (x) and (y) peaks originate from ZnS and ZnCdSe buffer layers, respectively.

Previously, the maximum etch rate of the MgS release layer from a GaAs/ZnSe/MgS/ZnSe sample was found to be about 3 mm/h.<sup>10</sup> In comparison, the etching rate for GaAs-based lift-off with an AlAs release layer is approximately 0.3 mm/h.<sup>11</sup> Typically, ZnSe/MgS/ZnSe samples are released from the buffer layer within about 30 min, but samples grown on InP etched much faster, with InP/ZnCdSe(60 nm)/

TABLE I. Lattice constants of the three substrates and lattice mismatch of ZnSe layers, together with the in plane strain measured by X-ray diffraction at 300 K and the calculated strain at the growth temperature.

	GaP	GaAs	InP
$a_{\text{sub}}$ (nm)	0.5451	0.5653	0.586
Lattice mismatch to ZnSe	$-3.8 \times 10^{-2}$	$-3 \times 10^{-3}$	$3.4 \times 10^{-2}$
Measured strain at 300 K	$1 \times 10^{-3}$	$-2 \times 10^{-3}$	$1 \times 10^{-3}$
Calculated layer strain at growth temperature	$-3 \times 10^{-4}$	$-1.9 \times 10^{-3}$	$5 \times 10^{-4}$

TABLE II. Graph of PL peak positions, and FWHM for ZnSe layers before and after ELO. Strains are given both at room temperature and at the growth temperature for the layer before ELO. PL transitions are assigned to light holes for tensile (positive) strains and heavy holes for compressive (negative) strains.

	GaP	GaAs	InP
<i>PL from epitaxial layer</i>			
ZnSe peak position (eV)	2.7879	2.7889	2.7795
Strain (PL) at 77 K	$-1.0 \times 10^{-2}$	$-1.1 \times 10^{-2}$	$-1.6 \times 10^{-3}$
Calculated strain at growth temperature	$-1.3 \times 10^{-3}$	$-1.7 \times 10^{-3}$	$1.4 \times 10^{-5}$
<i>PL from lifted layer</i>			
ZnSe peak position (eV)	2.7428	2.7496	2.7668
FWHM (meV)	36.19	33.36	22.6
Strain (PL) at 77 K	$5.7 \times 10^{-3}$	$4.6 \times 10^{-3}$	$1.8 \times 10^{-3}$

MgS(7 nm)/ZnCdSe(300 nm) layers etching in only 2 min, while the corresponding structures in the second set with a ZnSe capping layer etched in 4 min. In contrast, layers grown on GaP etched very slowly, taking about 24 h to lift the ZnSe epilayer from GaP/ZnS/MgS(7 nm)/ZnSe structure. Samples with a thick ZnS capping layer were even more difficult to etch. In this case, about 48 h was required before the wax cap separated from the layer. Unlike the other capping materials, ZnS does react slowly with HCl. Etching of the cap layer from the lower (MgS side) will occur but it is also possible that the junction between the wax and ZnS layer is affected causing the cap to detach without the film. The exact cause here is not known, but certainly in these samples there was no evidence of a lifted layer and the ZnS/MgS/ZnS layers were not investigated further.

For the ZnS/MgS/ZnSe samples, the interaction of the etch solution with the ZnS layer is a parasitic reaction which reduces the concentration of hydrogen ions in solution while simultaneously increasing the concentration of hydrogen sulphide. Although the reaction with ZnS is far slower than with MgS, the reduced etch rate is compensated by the larger etching surface, meaning that a significant quantity of hydrogen sulphide can be evolved. This effect must contribute to the reduced etch rate of the ZnSe layers grown on ZnS, but may not be the only effect. In addition, it cannot explain the significantly increased etch rate in layers deposited on InP. The model of ELO etching proposed by Yablonovich<sup>2</sup> suggests that the maximum possible etch rate should be limited by the solubility of the gaseous reaction product. A comparison of the solubilities of hydrogen (produced during the etching of AlAs) and hydrogen sulphide (in the present case) gives an estimate of the maximum etch rate for MgS as  $\sim 300$  times higher than for AlAs layers of comparable thickness.<sup>10</sup> This is approximately the rate observed in the fastest etching structures, which are grown on InP which suggests that the etch rates for all other samples have been reduced, including those grown on GaAs.

Another factor contributing to the reduction in etch rate may be the dependence on  $d$ , the thickness of the MgS layer. In II–VI structures grown on GaAs, the etch rate has been found to vary as  $d^{-1/2}$  in the thickest layers, as predicted by Yablonovich. However, there is a maximum etch rate which

is found in layers where  $d = 5\text{--}10$  nm, and in thinner layers the etch rate decreases sharply, becoming almost zero for  $d < 3$  nm. We have previously suggested that this is caused by strong dispersion forces holding the layers on either side of the MgS together, which prevents the free transport of reagents and products, thereby stopping etching.<sup>10</sup> In the present set of samples, all MgS layers had the same nominal thickness, but this will be reduced by any interdiffusion. In the case of ZnSe/MgS structures, previous X-ray interference studies have shown that a limited amount of intermixing does occur, with ZnMgSSe layers a few monolayers thick forming at each interface.<sup>12,13</sup> The ZnMgSSe phase diagram is known to have a region of immiscibility,<sup>14</sup> and the observed restricted amount of intermixing of ZnSe/MgS is in line with this. Significantly, there is no miscibility gap in the ternary ZnMgS system and in this case much larger interdiffusion would be expected leading to a substantially smaller  $d$ , and we have recently observed MgS/ZnS intermixing in double crystal X-ray spectra from thin ZnS/MgS/ZnS heterostructures.<sup>8</sup>

A full calculated phase diagram for CdMgSSe has not been published, but using the same model as used previously for ZnMgSSe,<sup>14</sup> it is found that the region of miscibility is drastically reduced to the percent level. CdSe and MgS are effectively immiscible, giving sharp boundaries between layers and a larger  $d$  for the same amount of deposited material. For the three substrates for the same nominal thickness of MgS, we predict that the actual layer thicknesses are  $d_{\text{GaP}} < d_{\text{GaAs}} < d_{\text{InP}}$ , which gives etch rates in the correct order for  $d < 10$  nm.

To determine whether the layer thickness made any contribution to the observed etch rate, a new set of samples were grown on GaP with a nominal  $d = 15$  nm using identical growth conditions and ELO procedure as before. This time the ZnS/MgS/ZnSe samples were lifted within  $\sim 2$  h.

After ELO, the released layers were placed on glass substrates and bonded by applying light pressure. The glass substrates are optically flat with surface roughness less than a quarter wavelength at 633 nm. After overnight drying, the wax was removed by dissolving it in 1-Bromopropane. All the epitaxial layers bonded strongly without adhesive through the van der Waals interaction.<sup>2</sup> Images taken using an optical microscope at 1000 $\times$  magnification ( $280 \times 210 \mu\text{m}^2$  area) show that, under ideal lift-off conditions, the surface of the lifted material after deposition on glass is virtually identical to the material prior to the lift-off. Although only 200–300 nm thick, the epitaxial layers were crack-free over square millimeter areas. Any cracks or other macroscopic defects are mostly related to the presence of small dust particles at the glass/semiconductor interface, as this work was carried out in a laboratory with an unfiltered air supply.

Fig. 3 shows the room temperature absorption spectra from the three ZnSe layers after ELO, which were grown on GaAs, GaP, and InP substrates. These spectra all exhibit a sharp decrease in transmittance at the band edge, with well resolved fringes below the bandgap showing that the layers are optically flat. A ZnSe band gap of approximately 2.7 eV is obtained from all the three ZnSe layer spectra. Similar



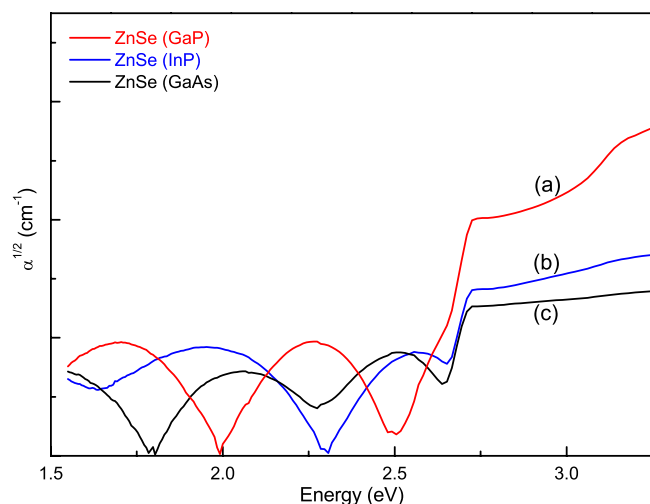


FIG. 3. Room Temperature absorption spectra of ZnSe epitaxial layers lifted-off from GaP, GaAs, and InP substrates.

absorption spectra (not shown) were obtained from ZnCdSe layers lifted from InP substrates and transferred to glass. A band gap of 2.4 eV was obtained from ZnCdSe epilayers and the fringes below bandgap again confirm that the films are of good optical quality after ELO.

77 K PL spectra were obtained from the ZnSe epilayers from set 2 before and after ELO. In the majority of cases, after lift off the PL intensity is reduced, typically by an order of magnitude. The most likely cause of this is that in ZnSe, PL emission is weak from the region immediately below the surface where there is strong band bending. After ELO, the number of free surfaces is doubled and the size of the emitting region is significantly reduced.

Fig. 4 shows a comparison of the 77 K PL spectra from ZnSe epilayers grown on GaP before ELO and from the ZnSe layer after ELO and transfer to a glass substrate. In this figure, the two ZnSe peaks have been normalized to the same intensity for clarity. In the case of the ZnS/MgS/ZnSe

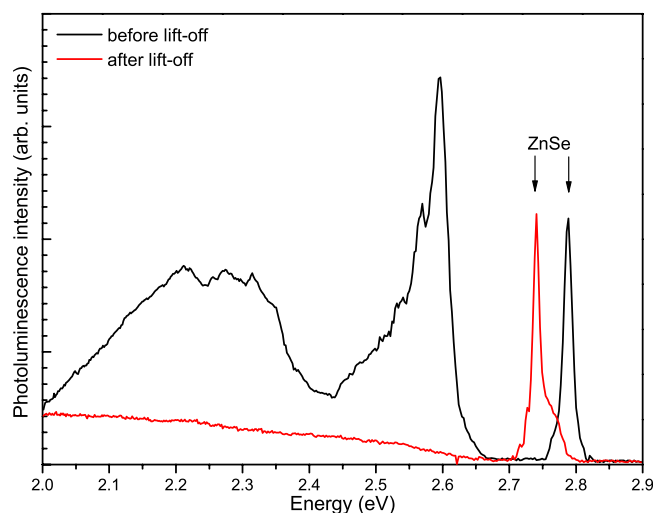


FIG. 4. Photoluminescence at 77 K from a GaP/ZnS/MgS/ZnSe heterostructure before ELO and from the top ZnSe layer after ELO and deposition on glass. The intensities of the ZnSe peaks have been normalized for comparison.

heterostructure before ELO, the top ZnSe layer is the only part of the MBE grown structure which has a bandgap smaller than the irradiating photon energy. The observable features in this spectrum correspond to those observed previously in epitaxial ZnSe layers deposited on GaAs substrates grown by both ourselves and others, and are very similar to the spectra seen from the layers in this study deposited on both GaAs and InP substrates. All three spectra show a broad peak around 2.2–2.3 eV, denoted the S band, previously assigned to either impurity or defect related luminescence<sup>15</sup> and the more intense, sharper Y-line at 2.6 eV together with its LO phonon replicas arising from misfit dislocations.<sup>16</sup> For the sample shown in Figure 3, the position of the S band overlaps that of the observed similarly broad near bandedge emission from the GaP substrate.<sup>17</sup> Therefore, a contribution to this peak from the fraction (approximately 20%–25%) of incident radiation which reaches the substrate cannot be ruled out. For the samples grown on GaAs and InP, this is not the case and there is no contribution from the substrate to the strong emission in this region.

The prominent peak seen in Figure 3 before ELO at  $\sim 2.75$  eV arises from near band edge emission from the ZnSe epilayers. In the sample shown, the Y line is more intense than the near band edge emission, suggesting the structure has a high density of misfit dislocations, as confirmed by almost complete relaxation found by the X-ray double crystal measurements given in Table II.

After ELO, the spectrum from the ZnSe layer is very different with a noticeable shift in the energy of the near band edge emission of  $\sim 50$  meV. It is also noticeable that the other spectral features have almost disappeared from the lifted layer, in particular, the Y line. If the dislocations producing the Y line were not located within the ZnSe layer, but immediately below it, either in the thin MgS or the ZnS layer, then after ELO they would be removed from the sample. However, both these layers have smaller strain thickness products than the ZnSe and are therefore less likely to relax. It is more likely that the dislocations are located within the ZnSe layer, and a more likely explanation is that, although present in the lifted layer, they are no longer optically active as they now lie within the depletion region extending in from the new lower surface of the sample. The S band emission around 2.2–2.3 eV is also much reduced in intensity in all samples. Any emission in this spectral region arising from a GaP substrate would be removed following ELO. In addition, for all samples ZnSe defect related emission is also predominantly from the same regions as the Y line emission, and is reduced accordingly.

In all ZnSe samples, one or more peaks can be identified as arising from free and donor bound emissions, although the resolution of the PL system is such that free excitonic and donor bound peaks overlap and contribute to one overall peak. The positions of the main PL peaks for the ZnSe layers both before and after ELO are given in Table II. This overall peak envelope changes after lift off signifying a change in the ratio of emission intensities from free and donor bound excitons. Again, the loss of emission from the region of the sample adjacent to the new free surface could cause this effect.

In all cases, there is a clear shift in the position of the main peak to lower emission energies after lift off, which is typically much larger than the energy resolution of the system. The likely origin of the peak shifts is changes in strain with the ZnSe layer, and it is possible to calculate the strain from the PL peak position assuming tetragonal distortion of the layer. However, in low resolution spectra this analysis requires the relative contributions of the free and donor bound excitonic peaks to remain roughly constant. A change in the ratio of the peak intensities does occur in some of the ZnSe samples studied here. However, assuming that the main peak derives from free excitonic emission, means that any change in the peak position derives only from changes in strain. This simplification allows an upper bound to be estimated for the strain.

Strains for the lifted and unlifted samples are given in Table II. For the ZnSe layers before ELO, they are in reasonable agreement with the corresponding strains determined from X-ray diffraction given in Table I. After ELO, the PL peaks from all layers are shifted to lower emission energies, which indicates a change from compressive to tensile strain, but there are significant differences between the three layers. ZnSe layers deposited on InP experience large tensile strain, and are completely (98%–100%) relaxed before lift off. After ELO there is little change in strain and the sample remains over 95% relaxed.

Samples grown on both GaP and GaAs substrates are under compressive strain and relax before lift off. In the samples grown on GaP, the larger initial strain means the relaxation is 97%–99% complete before ELO, while for the samples grown on GaAs the relaxation is only partial, in the range 30% (X-ray) to 37% (PL), respectively. In both cases, there are moderate tensile strains after lift off. A possible origin of the change of strain might be the difference in thermal expansion coefficients of ZnSe and glass substrates used. However, previous work on ZnMgSSe/ZnSe ELO structures, which were also transferred to glass, did not observe a PL peak shift which could be attributed to the glass,<sup>18</sup> which was thought to be due to the weak adhesion between the semiconductor and the new substrate. In addition, the PL peak shifts should be similar for all lifted samples. This is obviously not the case, which is almost zero change for the sample deposited on InP.

These samples are clearly not identical, and the differences may arise from the types of dislocation they contain and their distribution within the samples. It should be emphasized that these layer thicknesses were chosen to optimize the X-ray signal strength and the relaxation observed is an inevitable consequence of that choice. Significantly, the samples grown on GaAs are only partially relaxed, and the dislocation distribution in the ZnSe epilayers is higher at the ZnSe/GaAs interface.<sup>19,20</sup> This means that before ELO part of the ZnSe layer is still compressively strained. After removing the substrate, the layer lowers its total strain energy by reducing the compressive strain in this part of the layer while simultaneously introducing tensile strain in the previously relaxed part of the layer. This balancing of the strain states in unrelaxed II–VI multilayer structures with much smaller compressive and tensile strains has previously

been seen in previous ELO samples grown on GaAs substrates.<sup>18</sup> For the samples used in the present study, the residual strain in the optically active part of the ZnSe layer after ELO is now tensile.

The samples grown on InP substrates relax almost completely during growth, but unlike the samples grown on GaP, the initial strain state is compressive. As the relaxation mechanisms for tensile and compressive strains in III–V semiconductors utilize different dislocation types,<sup>21,22</sup> after relaxation the samples presumably contain completely different distributions of dislocations and residual strain states. There will still be small residual strains due to work hardening, meaning that could be a strain distribution in the samples grown on InP similar to that found in the samples grown on GaAs. Compared to the initial compressive strain in the ZnSe layer grown on InP before relaxation, the residual tensile strain is quite small, of order approximately 15% of its magnitude.

#### IV. CONCLUSION

In conclusion, we have demonstrated the use of thin ZB MgS epilayers as an effective sacrificial layer for epitaxial lift-off for layers deposited on GaP, GaAs, and InP. Different II–VI semiconductors, either lattice matched to the substrates or the ZB MgS were successfully lifted-off all three substrates. For layers deposited on GaAs and InP substrates, ELO can be performed in a few hours with high yield on large areas of material using ZB MgS layers only 7 nm thick. In the case of GaP substrates, a fast reproducible process is obtained by increasing the MgS layer thickness to 15 nm. The lifted epilayers have been structurally and optically characterized and no structural damage has been introduced to the lifted layer by the ELO process. Changes in the PL peak positions are observed, which are attributed to small changes in the strain state of the samples after ELO.

<sup>1</sup>M. Konagai, M. Sugimoto, and K. Takahashi, *J. Cryst. Growth* **45**, 277 (1978).

<sup>2</sup>E. Yablonovitch, T. Gmitter, J. P. Harbison, and R. Bhat, *Appl. Phys. Lett.* **51**, 2222 (1987).

<sup>3</sup>I. Pollentier, P. Demeester, A. Ackaert, L. Buydens, P. Van Daele, and R. Baets, *Electron. Lett.* **26**, 193 (1990).

<sup>4</sup>E. Yablonovitch, E. Kapon, T. Gmitter, C. Yun, and R. Bhat, *IEEE Photon. Technol. Lett.* **1**, 41 (1989).

<sup>5</sup>K. Weber, A. Blakers, and K. Catchpole, *Appl. Phys. A: Mater. Sci. Process.* **69**, 195 (1999).

<sup>6</sup>C. Brys, F. Vermaerke, P. Demeester, P. V. Daele, K. Rakennus, A. Salokatve, P. Uusimaa, M. Pessa, A. L. Bradley, J. P. Doran, J. O'Gorman, and J. Hegarty, *Appl. Phys. Lett.* **66**, 1086 (1995).

<sup>7</sup>A. Balocchi, A. Curran, T. C. M. Graham, C. Bradford, K. A. Prior, and R. J. Warburton, *Appl. Phys. Lett.* **86**, 011915 (2005).

<sup>8</sup>A. Rajan, R. T. Moug, and K. A. Prior, *Appl. Phys. Lett.* **102**, 032102 (2013).

<sup>9</sup>I. Davidson, R. Moug, E. Vallance, M. Tamargo, and K. Prior, *Phys. Status Solidi A* **209**, 1428 (2012).

<sup>10</sup>A. Curran, S. Brown, R. Warburton, and K. Prior, *Phys. Status Solidi B* **247**, 1399 (2010).

<sup>11</sup>J. Schermer, P. Mulder, G. J. Bauhuis, M. M. A. J. Voncken, J. van Deelen, E. Haverkamp, and P. K. Larsen, *Phys. Status Solidi A* **202**, 501 (2005).

<sup>12</sup>C. Bradford, C. B. O'Donnell, B. Urbaszek, A. Balocchi, C. Morhain, K. A. Prior, and B. C. Cavenett, *Appl. Phys. Lett.* **76**, 3929 (2000).

- <sup>13</sup>K. Prior, X. Tang, C. O'Donnell, C. Bradford, L. David, and B. Cavenett, *J. Cryst. Growth* **251**, 565 (2003).
- <sup>14</sup>V. Sorokin, S. Sorokin, V. Kaygorodov, and S. Ivanov, *J. Cryst. Growth* **214–215**, 130 (2000).
- <sup>15</sup>J. Gutowski, N. Presser, and G. Kudlek, *Phys. Status Solidi A* **120**, 11 (1990).
- <sup>16</sup>S. Myhajlenko, J. L. Batstone, H. J. Hutchinson, and J. W. Steeds, *J. Phys. C: Solid State Phys.* **17**, 6477 (1984).
- <sup>17</sup>T. Yu, T. Matsuo, K. Suto, and J. Nishizawa, *J. Electron. Mater.* **28**, 1101 (1999).
- <sup>18</sup>R. Moug, C. Bradford, A. Curran, F. Izdebski, I. Davidson, K. Prior, and R. J. Warburton, *Microelectron. J.* **40**, 530 (2009).
- <sup>19</sup>J. Ayers, *J. Appl. Phys.* **78**, 3724 (1995).
- <sup>20</sup>S. Kalisetty, M. Gokhale, K. Bao, J. Ayers, and F. Jain, *Appl. Phys. Lett.* **68**, 1693 (1996).
- <sup>21</sup>P. Maree, J. Barbour, J. van der Veen, K. Kavanagh, C. T. Bulle-Lieuwma, and M. Vieggers, *J. Appl. Phys.* **62**, 4413 (1987).
- <sup>22</sup>G. Salviati, C. Ferrari, L. Lazzarini, L. Nasi, A. Drigo, M. Berti, D. D. Salvador, M. Natali, and M. Mazzer, *Appl. Surf. Sci.* **188**, 36 (2002).